J Clin Periodontol 2005; 32: 104–110, doi: 10.1111/j.1600-051X.2004.00632.x

Journal of Clinical Periodontology

Periodontal repair in dogs: guided tissue regeneration enhances bone formation in sites implanted with a coral-derived calcium carbonate biomaterial

Ki-Tae Koo[1], Giuseppe Polimeni[1], Mohammed Qahash[1], Chong Kwan Kim[2] and Ulf ME Wikesjö[1]

[1]Laboratory for Applied Periodontal and Craniofacial Regeneration, Department of Periodontology, Temple University School of Dentistry, Philadelphia, PA, USA; [2]Research Institute for Periodontal Regeneration, Department of Periodontology, Yonsei University College of Dentistry, Seoul, Korea

Koo K-T, Polimeni G, Qahash M, Kim CK, Wikesjö UME: Periodontal repair in dogs: guided tissue regeneration enhances bone formation in sites implanted with a coral-derived calcium carbonate biomaterial. J Clin Periodontol 2005; 32: 104–110. doi: 10.1111/j.1600-051X.2004.00632.x. © Blackwell Munksgaard, 2004.

Abstract

Background: Previous studies suggest that a bioresorbable calcium carbonate coral implant (CI) supports space provision and bone formation for guided tissue regeneration (GTR). However, it could not be discerned whether observed effects were because of GTR or whether the CI possessed osteoconductive properties enhancing bone formation. The objective of this study was to evaluate bone formation associated with the CI biomaterial in the presence and absence of provisions for GTR.

Methods: Routine, critical size, 6 mm, supra-alveolar periodontal defects were created in 12 young adult Beagle dogs. Five animals received the CI alone (Biocoral® 1000). Seven animals received the CI/GTR combination using an expanded polytetrafluoroethylene barrier (GORE-TEX® Regenerative Material). The animals were euthanized at 4 weeks postsurgery and tissue blocks of the experimental sites were collected and processed for histometric analysis.

Results: Clinical healing was uneventful. The histopathologic and histometric analysis revealed significantly increased bone formation (height and area) in sites receiving the CI/GTR combination compared with CI alone (2.3 ± 0.6 versus 1.2 ± 0.9 mm; and 3.1 ± 0.8 versus 1.2 ± 1.1 mm^2; $p < 0.05$). The CI biomaterial appeared to be mostly unassociated with new bone formation; the CI particles were observed sequestered in newly formed bone, fibrovascular marrow, and in the supra-alveolar connective tissue. Cementum formation was limited and observed in few sites for both treatment protocols.

Conclusion: While GTR promoted new bone formation, the CI contributed limited, if any, osteoconductive effects.

Key words: bone regeneration; coral biomaterial; dogs; guided tissue regeneration; tissue engineering

Accepted for publication 14 April 2004

The success and efficacy of guided tissue regeneration (GTR) therapy using barrier devices have been shown to be dependent on the space-providing capacity of the device (Haney et al. 1993, Sigurdsson et al. 1994). Failure to provide space has resulted in impaired or hindered regeneration. Collapse or compression of the barrier device into a periodontal defect or onto the root surface will necessarily compromise migration and proliferation of cells from the periodontal ligament. In other words, the device becomes a physical obstacle to bone and cementum regeneration. Numerous attempts have been made to overcome this limitation. For example, structurally reinforced barriers have been developed to facilitate space maintenance for GTR (Sigurdsson et al. 1994, Tinti & Vincenzi 1994, Cortellini et al. 1995).

Various osteogenic, osteoconductive, and osteoinductive implants including autogenous bone, bone derivatives, and bone substitutes have been suggested to support regeneration of alveolar bone, and for some biomaterials the periodontal attachment (Mellonig 1996, Nasr et al. 1999). Another rationale for using

bone grafts or bone biomaterials has been to secure space provision for GTR. Conceptually, however, these same biomaterials may obstruct the wound space to migration and proliferation of cells from the periodontal ligament and the alveolar bone.

Previous studies suggest that a bioresorbable calcium carbonate coral implant (CI) supports space provision and bone formation for GTR (Wikesjö et al. 2003a). However, it could not be discerned whether the observed effects were because of GTR or whether the CI possessed osteoconductive properties enhancing bone formation. The objective of this study was to evaluate bone formation associated with the CI biomaterial in the presence and absence of provisions for GTR.

Material and Methods

Animals

Animal selection and management, and surgical protocol followed routines approved for this study by the Institutional Animal Care and Use Committee, Loma Linda University, CA, USA. Twelve male Beagle dogs (age 18–24 months, weight 12–15 kg) exhibiting intact mandibular premolar dentition without crowding or evidence of periodontal disease were used.

Biomaterials

Expanded polytetrafluoroethylene (ePTFE) barriers (GORE-TEX® Regenerative Material Transgingival Configuration, W.L. Gore & Associates Inc., Flagstaff, AZ, USA) were used. ePTFE sutures (GORE-TEX® Suture CV5, W.L. Gore & Associates Inc.) were used for barrier fixation and wound closure.

A medical-grade, resorbable, porous, particulate, calcium carbonate CI (Biocoral® 1000, Inoteb, Saint-Gonnery, France) was used. The CI was combined with a medical-grade binding material that provided beneficial handling characteristics; hydroxyethyl starch was mixed with 0.5% gelatin and a 20 μM sodium acetate solution to form a viscoelastic gel to contain the calcium carbonate particles in a manageable mass.

Surgical protocol

Food was withheld the night before surgery. Surgical procedures were performed using sodium pentobarbital anesthesia (20–30 mg/kg, i.v.) preceded by acepromazine sedation (1 mg/kg, i.m.). Routine dental infiltration anesthesia was used at the surgical sites. To maintain hydration, a sterile i.v. catheter was placed and animals received a constant rate infusion (10–20 ml/kg/h i.v.) of lactated Ringer's solution while anesthetized. Thiopental sodium anesthesia (20–25 mg/kg, i.v.) was used for suture removal and radiographic registrations.

The maxillary first, second, and third premolar teeth were surgically extracted, and the maxillary fourth premolars were reduced in height and exposed pulpal tissues were sealed (Cavit®, ESPE, Seefeld/Oberbayern, Germany) to alleviate potential mechanical trauma from the maxillary teeth to the experimental sites postsurgery.

Supra-alveolar, critical size, periodontal defects were created around the third and fourth mandibular premolar teeth in the right and left jaw quadrants in each animal (Fig. 1; Wikesjö et al. 1994). Briefly, buccal and lingual mucoperiosteal flaps were reflected following buccal and lingual sulcular incisions from the canine tooth to the second molar. The alveolar bone was removed to approximately 6 mm apical to the cemento-enamel junction (CEJ) of the premolar teeth. The first and second premolars were extracted, and the first molar was amputated to the

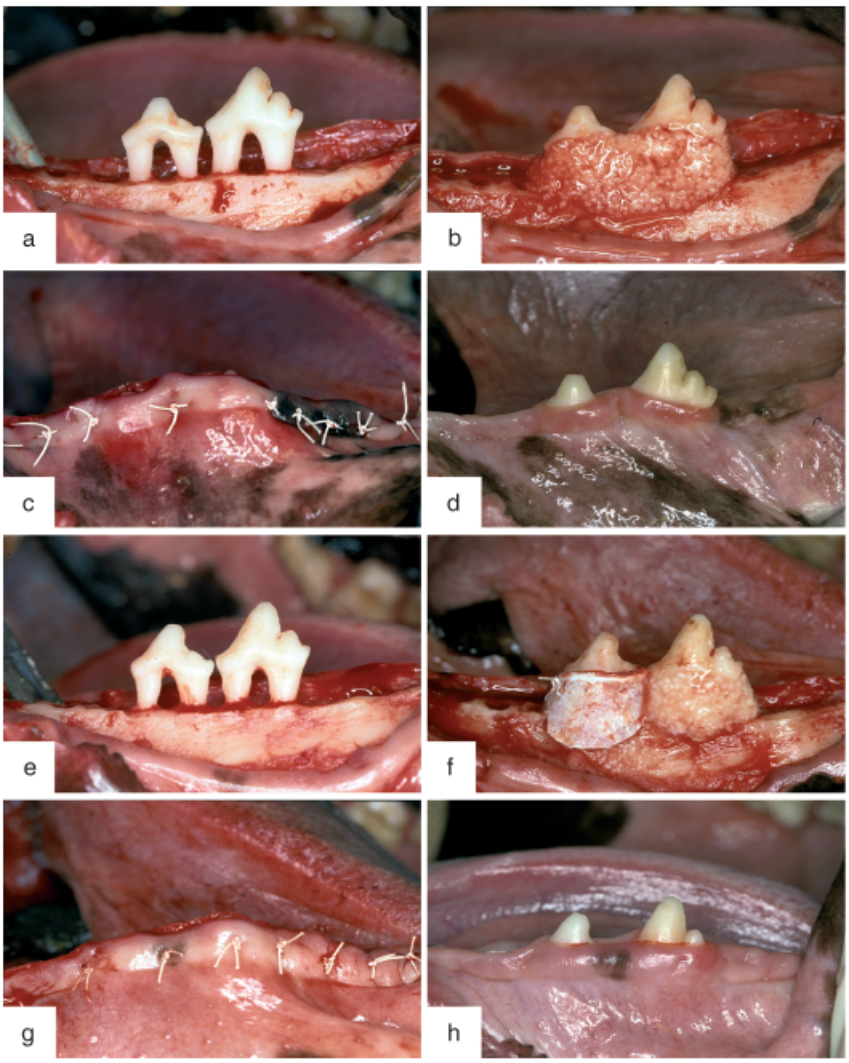

Fig. 1. Critical size, supra-alveolar periodontal defects were created around the third and fourth mandibular premolar teeth. The alveolar bone was removed to approximately 6 mm apical to the cemento-enamel junction of the premolar teeth (a, e). One defect site is implanted with coral implant (CI) (b), and the other site with CI/GTR (f). Gingival flaps were advanced for transgingival wound closure (c, g). Healing at 4 weeks was generally uneventful. Exposures of the expanded polytetrafluoroethylene barrier were not observed (d, h). GTR, guided tissue regenaration.

level of the surgically reduced alveolar bone. The root surfaces were instrumented with curettes, chisels, and water-cooled rotating diamonds to remove the cementum.

Experimental protocol

Experimental conditions included implantation of the CI in one jaw quadrant in each of five animals. Seven animals received the CI in combination with GTR in one jaw quadrant. Experimental conditions were alternated between left and right jaw quadrants in subsequent animals. Contralateral jaw quadrants were used for other experiments reported elsewhere.

Defects receiving the CI had the implant molded around the premolar teeth to replace removed alveolar bone (actual implant volume/defect approximated 0.8 ml). Animals that additionally received GTR were each fitted with an ePTFE barrier positioned and secured with an ePTFE suture immediately above the CEJ. Periostea were fenestrated at the base of the flaps, the flaps were advanced, and the flap margins were adapted and sutured approximately 2 mm coronal to the ePTFE barrier (Fig. 1).

Postsurgery protocol

Buprenorphine HCl (0.015 mg/kg, i.m., b.i.d., 2 days) was administered for immediate postsurgery pain control. A broad-spectrum antibiotic (enrofloxacin, 2.5 mg/kg, i.m., b.i.d., 14 days) was used for infection control. Plaque control was maintained by twice daily topical application of a chlorhexidine solution (chlorhexidine gluconate; 40 ml of a 2% solution). Sutures were removed at 10 days postsurgery. The animals were anesthetized and euthanized (concentrated thiopental sodium i.v.) at week 4 postsurgery when teeth with surrounding soft and hard tissues were removed en bloc. The barriers were not removed. Observations of the experimental sites with regards to gingival health, flap adaptation, edema, and purulence were made daily.

Histological processing and evaluation

The block sections were fixed in 10% buffered formalin for 3–5 days, decalcified in 5% formic acid for 8–10 weeks, trimmed, dehydrated, and embedded in butyl-methacrylate-paraffin. Serial sections (7 μm) were cut in a buccal–lingual plane throughout the mesial–distal extension of the teeth. Every 14th section was stained with Ladewig's connective tissue stain modified by Mallory allowing for observations at 100 μm intervals.

The histopathologic evaluation by two examiners included observations of epithelial attachment, bone and cementum formation, formation of a periodontal ligament, presence and location of inflammatory reactions, position of the ePTFE barrier, presence and distribution of the CI biomaterial, bone formation associated with the biomaterial, and biomaterials resorption.

The most central stained section for the mesial and distal root of the third and fourth premolar teeth was identified by the size of the root canal. This section and the immediate stained step serial section on either side were subject to histometric analysis. Thus, three subsequent step serial sections, representing 0.2 mm of the mid-portion of the mesial and distal root for each premolar tooth, were used. One calibrated investigator, masked to the specific experimental conditions, performed the histometric analysis using incandescent and polarized light microscopy (BX 60, Olympus America, Inc., Melville, NY, USA), a microscope digital camera system (DP10, Olympus America, Inc.), and a PC-based image analysis system (Image-Pro Plus™, Media Cybernetic, Silver Springs, MD, USA) customized for the supra-alveolar periodontal defect model. The following parameters were recorded for the buccal and the lingual tooth surfaces for each section:

- *Defect height*: distance between the apical extension of the root planing and the CEJ.
- *Barrier height*: distance between the apical extension of the root planing and the most coronal aspect of the ePTFE barrier.
- *Defect area*: area under the ePTFE barrier circumscribed by the planed root, the width of the alveolar bone at the apical extension of the root planing, and the barrier.
- *Connective tissue repair*: distance between the apical extension of the root planing and the apical extension of a junctional epithelium along the planed root.
- *Cementum regeneration*: distance between the apical extension of the root planing and the coronal extension of a continuous layer of new cementum or cementum-like deposit on the planed root.
- *Bone regeneration* (*height*): distance between the apical extension of the root planing and the coronal extension of alveolar bone formation along the planed root.
- *Bone regeneration* (*area*): area represented by new alveolar bone along the planed root.
- *Bone regeneration* (*density*): ratio mineralized bone matrix/bone regeneration area.
- *Biomaterial density*: ratio residual biomaterial/bone regeneration area.
- *Root resorption*: combined linear heights of distinct resorption lacunae on the planed root.
- *Ankylosis*: combined linear heights of ankylotic unions between new alveolar bone and the planed root.

Data analysis

Summary statistics (mean $\pm$ SD) based on animal means were calculated using selected step serial sections. Differences between experimental conditions were analyzed using an unpaired *t*-test. Significance was accepted at a probability level of $p \leqslant 0.05$. Estimating the intraclass correlation coefficient assessed intraexaminer reproducibility.

Results

Clinical and radiographic observations

Healing was generally uneventful. Clinical appearance at sacrifice, at week 4 postsurgery, was similar for both experimental groups. Exposures of the ePTFE barrier were not observed. Gingival conditions appeared healthy (Fig. 1).

The defect sites exhibited radiopacity of granular nature consistent with the CI at 4 weeks postsurgery (not shown). The radiopacity varied within and between the treatment protocols. The CI/GTR group consistently demonstrated greater radiopacity than the CI group. Although the extent of the radiopacity varied, both groups appeared to retain a significant amount of the CI at week 4 postsurgery.

Histologic observations

All teeth were available for the histopathologic and histometric analyses. No obvious inflammatory infiltrates were observed. The junctional epithelium appeared to be arrested near or at the

CEJ in the CI/GTR group. In the CI group, the junctional epithelium was commonly arrested at the CEJ, but was also arrested apical to the CEJ.

Bone regeneration of trabecular nature appeared more extensive in the CI/GTR compared with the CI group (Figs 2 and 3). The newly formed woven bone included elements of lamellar bone. In more coronal aspects of the defects, in particular in the CI/GTR group, islands of bone formation surrounded by plump osteoblast-like cells were observed. Importantly, the newly formed bone appeared to be generally unrelated to the coral biomaterial.

The healing response to the CI appeared to be highly variable for both groups. CI particles were observed entrapped or sequestered within the newly formed bone, within fibrovascular marrow, and within the immediate connective tissue coronal and lateral to the newly formed bone (Figs 4 and 5). Commonly, the CI particles did not contact newly formed bone. Occasionally, CI particles were observed accumulated juxtaposed to the resident bone of the surgically reduced alveolar crest. More CI particles were retained within the newly formed bone and the immediate connective tissue in the CI/GTR than in the CI group (Figs 4 and 5). CI particles sequestered in the connective tissue were apparently undergoing resorption. The borders of the particles appeared scalloped, and some particles were observed surrounded by multinucleated cells, suggesting active resorption of the CI biomaterial (Figs 4 and 5). Other CI particles exhibited no apparent evidence of bioresorption.

Bone formation in relation to the CI biomaterial varied from animal to animal within and between groups. Also, bone formation varied considerably within the same animal, even between the buccal and lingual surfaces of the same root (Fig. 6). Whereas one surface could show extensive bone formation, the opposite surface exhibited limited, if any, newly formed bone. Cementum regeneration, limited to the very apical extension of the defect, was observed for both groups. Root resorption and ankylosis appeared to be insignificant for both groups.

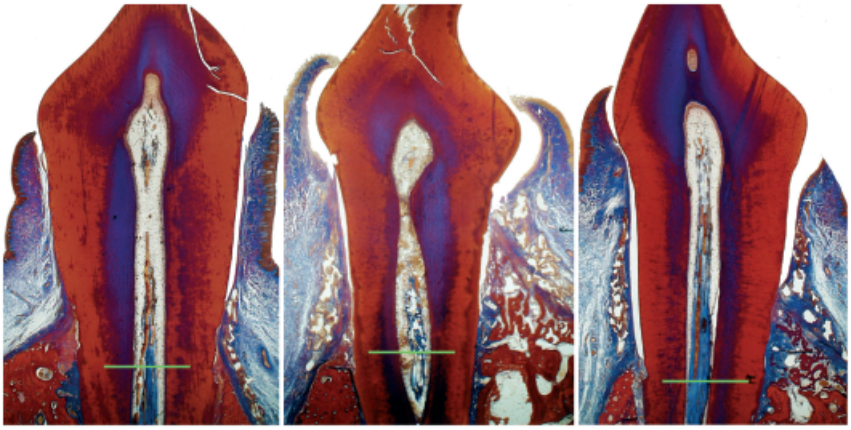

Fig. 2. Representative photomicrographs of teeth from three animals receiving CI only. The green line depicts the base of the defect. Note limited and variable bone formation and residual biomaterial sequestered in the connective tissue (original magnification $\times$ 2.5; Ladewig's connective tissue stain). CI, coral implant.

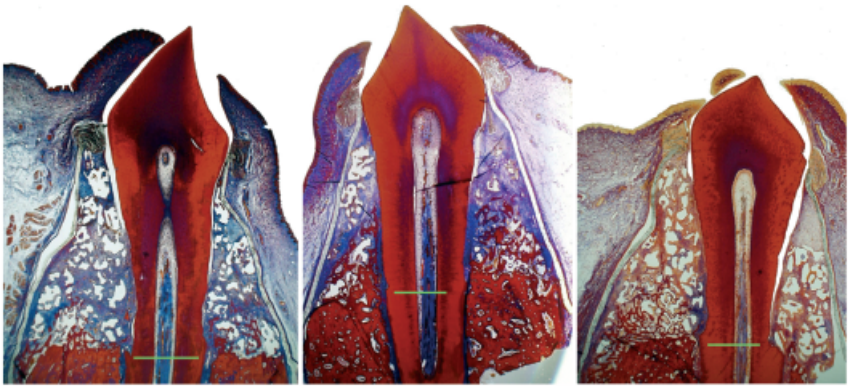

Fig. 3. Representative photomicrographs of teeth from three animals receiving CI/GTR. The green line depicts the base of the defect. Note more extensive bone formation and residual coral biomaterial than following use of CI only. New bone formation is variable from site to site. Extensive amounts of residual coral biomaterial is residing within the newly formed bone and fibrovascular marrow as well as in the peri-alveolar connective tissue (original magnification $\times$ 2.5; Ladewig's connective tissue stain). CI, coral implant; GTR, guided tissue regeneration.

Histometric analysis

Table 1 shows the results of the histometric analysis. Bone regeneration (height and area) was significantly greater for the CI/GTR compared with the CI group. Sites receiving the CI protocol exhibited a junctional epithelium averaging 0.4 ± 0.3 mm compared with 0.0 ± 0.0 mm for sites also receiving the ePTFE barrier ($p = 0.014$). Bone regeneration (height) amounted to 2.3 ± 0.6 versus 1.2 ± 0.9 mm for the CI/GTR and CI group, respectively ($p = 0.0355$). Bone regeneration (area) was twofold greater in sites receiving the CI/GTR compared with the CI protocol (3.1 ± 0.8 versus 1.2 ± 1.1 mm^2, $p = 0.0049$). The density of the CI biomaterial within newly formed bone was greater in the CI/GTR compared with that in the CI group ($13.7 \pm 3.8\%$ versus $8.1 \pm 1.7\%$; $p = 0.0114$). The intraexaminer reproducibility for the histometric evaluation was generally high (intraclass correlation coefficient ≥ 0.9; for details see Koo et al. 2004).

Discussion

The objective of this study was to evaluate bone formation associated with a CI biomaterial in the presence and absence of provisions for GTR. Critical size, supra-alveolar periodontal defects in 12 Beagle dogs received CI biomaterial alone or combined with GTR. The animals were euthanized at 4 weeks postsurgery and tissue blocks of the experimental sites were processed for histometric analysis. There was significantly greater bone formation in sites

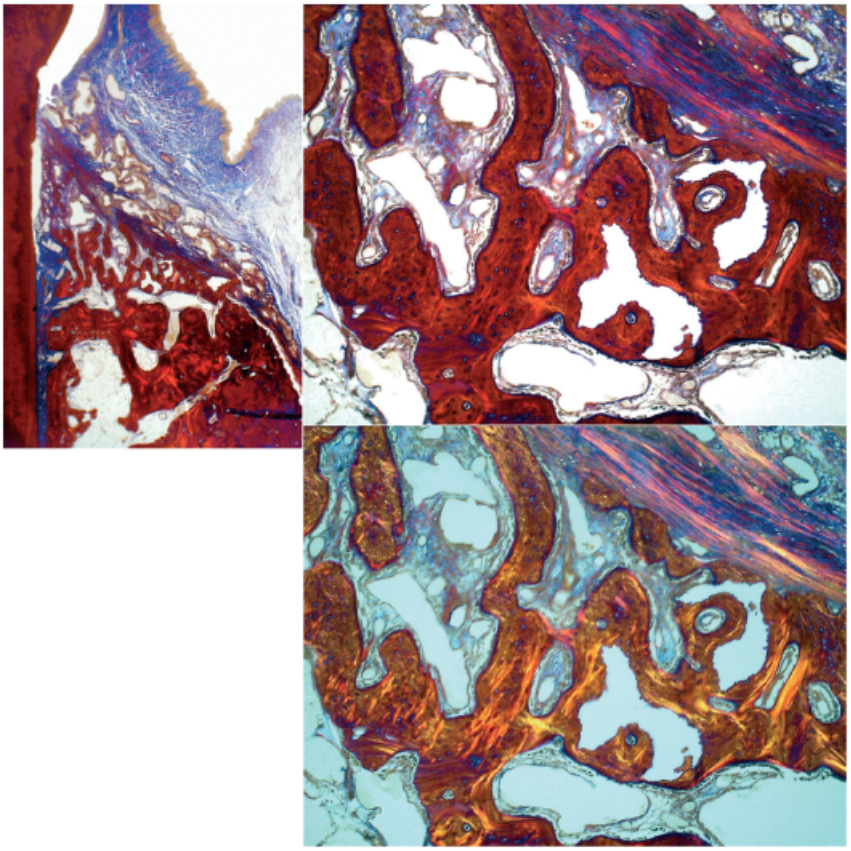

Fig. 4. Photomicrograph of defect site receiving CI only showing moderate new bone formation including woven bone and elements of lamellar bone. Extended aggregates of the coral biomaterial apparently undergoing active resorption are located immediately outside the newly formed bone. Coral particles can also be observed within the newly formed bone or fibrovascular marrow without apparent bone metabolic activity, i.e. presence of osteoblastic cells and osteoid formation or osteoclastic cells (original magnification × 4 (overview) and × 8; Ladewig's connective tissue stain; polarized light). CI, coral implant.

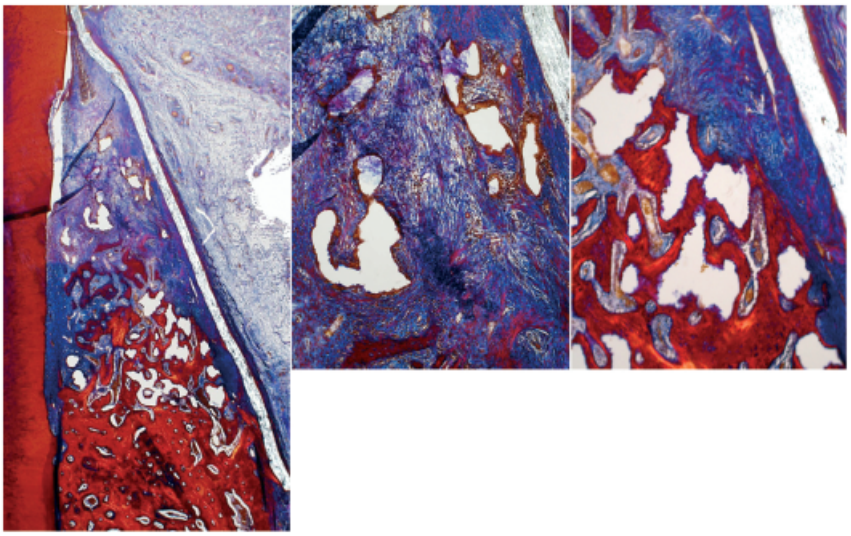

Fig. 5. Photomicrograph of defect site receiving CI/GTR showing moderate new bone formation including woven bone and elements of lamellar bone. Coral particles without apparent bone metabolic activity appear entrapped in bone or in the peri-alveolar connective tissue. Coral particles within the connective tissue are surrounded by multinucleated cells, suggesting active resorption of the biomaterial (original magnification × 4 (overview) and × 8; Ladewig's connective tissue stain). CI, coral implant; GTR, guided tissue regeneration.

receiving CI/GTR compared with CI alone. CI particles remained embedded in newly formed bone and fibrovascular marrow and connective tissue apparently unrelated to new bone formation.

The model used in this study is the critical size, supra-alveolar, periodontal defect model that has been presented in several previous reports (Wikesjö et al. 1994). Circumferential 6 mm periodontal defects were created around the third and fourth premolar teeth. The osteogenic potential in this defect model following sham surgery amounts to less than 20% of the defect height following a 4- or 8-week healing interval. Cementum regeneration is similarly limited following sham surgery. This challenging model appears to be suitable to evaluate the osteoconductive or osteoinductive capacity of bone derivatives like the CI biomaterial intended for periodontal reconstructive surgery or alveolar augmentation procedures.

The CI biomaterial used in this study, derived from the genus *Porites*, consists of resorbable aragonite crystals with an average pore size of 250 μm. When implanted into bone sites, fibrovascular tissue has been observed surrounding and within the porous structure of the CI, which, in turn, is gradually resorbed by osteoclasts and replaced by bone. The resorption of the coral biomaterial and osseous neo-formation appear variable according to the recipient site, the coral biomaterial used, the size of the implant, and the animal species. Bioresorption appears faster and more significant in more porous implants. Resorbable CIs of the genus *Porites* appear well tolerated and have been suggested to support bone regeneration in a variety of settings including posterolateral lumbar spinal fusion (Boden et al. 1997), repair of long bones (Guillemin et al. 1987, 1989, Gao et al. 1997), mandibular defects (Holmes 1979, Piattelli et al. 1997), and periodontal regeneration (Moon et al. 1996, Wikesjö et al. 2003a). In addition, CI implants have been used in combination with growth and differentiation factors in the reconstruction of defects in the craniofacial, axial, and appendicular skeleton (Boden et al. 1997, Wikesjö et al. 1998, Tatakis et al. 2000, Tuominen et al. 2000, Boyne & Shabahang 2001, Kujala et al. 2002).

Bone formation varied from animal to animal within and between groups. Bone formation also varied considerably within the same animal, even

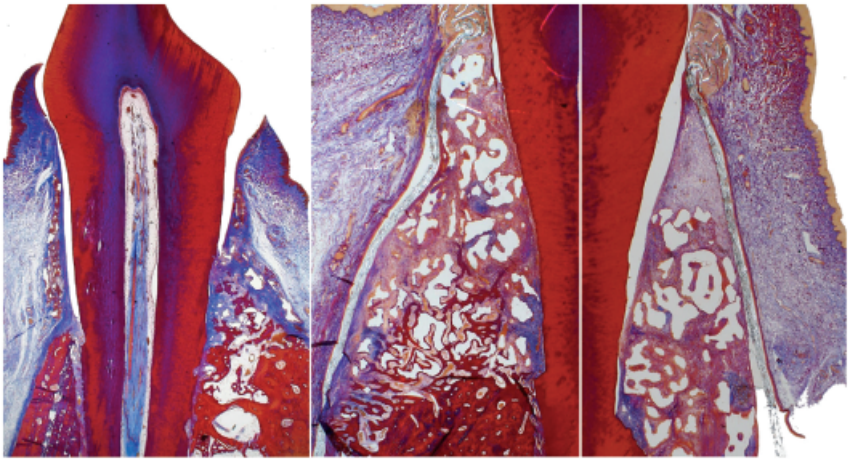

Fig. 6. Representative photomicrographs of defect sites receiving CI (left panel) or CI/GTR illustrating the unpredictability of bone formation associated with the CI biomaterial. Bone formation varied within and between animals and between groups (original magnification × 4; Ladewig's connective tissue stain). CI, coral implant; GTR, guided tissue regeneration.

Table 1. Summary statistics (group mean ± SD) for animals receiving CI versus animals receiving CI/GTR in mm (defect area, bone regeneration (area) in mm^2; bone regeneration (density) and biomaterial (density) in %)

	CI	CI/GTR	*p*-value CI versus CI/GTR
Defect height	4.7 ± 0.5	4.6 ± 0.6	0.6827
Barrier height	–	5.0 ± 0.6	–
Wound area	–	6.7 ± 1.5	–
Junctional epithelium	0.4 ± 0.3	0.0 ± 0.0	**0.014**
Connective tissue repair	4.3 ± 0.6	4.6 ± 0.6	0.4433
Cementum regeneration	0.002 ± 0.004	0.01 ± 0.02	0.4543
Bone regeneration (height)	1.2 ± 0.9	2.3 ± 0.6	**0.0355**
Bone regeneration (area)	1.2 ± 1.1	3.1 ± 0.8	**0.0049**
Bone regeneration (density)	23.1 ± 3.8	18.8 ± 5.0	0.1333
Biomaterial density	8.1 ± 1.7	13.7 ± 3.8	**0.0114**
Root resorption	0.1 ± 0.04	0.04 ± 0.06	0.1392
Ankylosis	0.2 ± 0.3	0.1 ± 0.1	0.2220

SD, standard deviation; CI, coral implant; GTR, guided tissue regeneration. bold values, p-value < 0.05

between the buccal and lingual surfaces of the same root. Whereas one surface showed extensive bone formation, the opposite surface exhibited limited, if any, evidence of newly formed bone. Overall, bone formation was significantly enhanced in the CI/GTR compared with the CI group. A twofold increase in bone height and area was observed in sites receiving the CI/GTR compared with the CI protocol. The mean vertical bone formation approximated 1.2 mm in sites receiving the CI implant alone. This should be compared with the osteogenic potential in sham-surgery controls in this model ranging from 0.5 to 2.4 mm (Wikesjö & Nilvéus 1991). Although direct comparisons between studies cannot be made, these observations from the same animal model suggest that the CI biomaterial has a limited osteoconductive effect.

The histopathologic evaluation in this study indicated that new bone formation in general appeared to be unrelated to the coral biomaterial. The CI particles did not appear to serve as a scaffold for enhanced bone formation. Previous studies suggest that when combined with GTR, the CI biomaterial enhanced space provision and bone formation compared with GTR alone (Wikesjö et al. 2003a); however, it has also been shown that this may be an effect of a space-providing property of the biomaterial and not one of osteoconductivity (Polimeni et al. 2004). Collectively, these observations suggest that the CI biomaterial has limited, if any, osteoconductive potential; in other words, the biomaterial does not enhance osteogenesis at the site. The histopathologic observations point to newly formed bone at times entrapping the CI particles. However, more commonly, the CI biomaterial was not associated with bone formation; the CI particles were observed sequestered in fibrovascular marrow and in the supra-alveolar connective tissue. These observations further suggest that the CI biomaterial has a limited osteoconductive potential.

The healing response to the CI biomaterial was highly variable within both groups. As mentioned above, the CI particles were observed entrapped or sequestered within newly formed bone, fibrovascular marrow, and the immediate connective tissue coronal and lateral to the newly formed bone. More CI particles were observed within the newly formed bone and the immediate connective tissue in the CI/GTR compared with the CI group. This could be an effect of the confinement by the GTR device delaying bioresorption and/or preventing migration of the biomaterial from the site. Indeed, occasionally, CI particles were observed accumulated juxtaposed to the surgically reduced alveolar crest, suggesting that the CI biomaterial had migrated. Regardless, the CI biomaterial was apparently undergoing bioresorption. CI particles exhibited scalloped borders and particles were observed surrounded by multinucleated cells. Still other particles exhibited no apparent evidence of bioresorption, suggesting that resorption of the biomaterial may take a long time, which should be considered when this biomaterial is to be used for bone augmentation procedures.

The objective of this study was to evaluate the osteoconductive effect of a CI biomaterial in a discriminating animal model with limited osteogenic potential. Nevertheless, the analysis also included observations of other healing parameters. Whereas a limited aspect of the CI sites exhibited formation of an epithelial attachment, the epithelium was arrested at the CEJ in sites following the CI/GTR protocol. This observation is in concordance with previous studies suggesting that GTR devices may support wound stability and formation of a connective tissue attachment eventually maturing into cementum and a functionally oriented periodontal ligament (Haney et al. 1993, Sigurdsson et al. 1994, Wikesjö et al 2003b–d).

Cementum regeneration was limited following the 4-week healing interval. Previous studies in this and similar animal models suggest that observations

of appreciable cementum formation using light microscopy may not be possible as early as 4 weeks postsurgery (Haney et al. 1993, Moon et al. 1996, Trombelli et al. 1999, Wikesjö et al. 1998, 2003a, Tatakis et al. 2000). Moon et al. (1996) suggested that cementum formation might be observed within a 6-week healing interval. Indeed, significant regeneration of the periodontal attachment encompassing up to 94% of the defect height has been observed at 8 and 24 weeks postsurgery in the supraalveolar defect model following GTR procedures (Sigurdsson et al. 1994, Wikesjö et al. 2003b–d). Therefore, longer healing intervals appear necessary when the objective of the study includes evaluation of periodontal regeneration.

In summary, bone formation was significantly enhanced in sites receiving CI/GTR. Bone formation appeared to be unrelated to the CI biomaterial; the CI remained in situ at 4 weeks sequestered in bone, fibrovascular marrow, and connective tissue. Cementum regeneration was limited; thus, longer healing intervals appear necessary to evaluate periodontal regeneration in this defect model. Ankylosis and root resorption were rare observations.

Conclusion

While GTR promoted new bone formation, the CI contributed limited, if any, osteoconductive effects.

References

Boden, S. D., Schimandle, J. H., Hutton, W. C., Damien, C. J., Benedict, J. J., Baranowski, C. & Collier, S. (1997) In vivo evaluation of a resorbable osteoinductive composite as a graft substitute for lumbar spinal fusion. *Journal of Spinal Disorders* **10**, 1–11.

Boyne, P. J. & Shabahang, S. (2001) An evaluation of bone induction delivery materials in conjunction with root-form implant placement. *The International Journal of Periodontics & Restorative Dentistry* **21**, 333–343.

Cortellini, P., Prato, P. G. & Tonetti, M. S. (1995) Periodontal regeneration of human intrabony defects with titanium reinforced barriers: a controlled clinical trial. *Journal of Periodontology* **66**, 797–803.

Gao, T. J., Tuominen, T. K., Lindholm, T. S., Kommonen, B. & Lindholm, T. C. (1997) Morphological and biomechanical difference in healing in segmental tibial defects implanted with Biocoral or tricalcium phosphate cylinders. *Biomaterials* **18**, 219–223.

Guillemin, G., Meunier, A., Dallant, P., Christel, P., Pouliquen, J. C. & Sedel, L. (1989) Comparison of coral resorption and bone apposition with two natural corals of different porosities. *Journal of Biomedical Materials Research* **23**, 765–779.

Guillemin, G., Patat, J. L., Fournie, J. & Chetail, M. (1987) The use of coral as a bone graft substitute. *Journal of Biomedical Materials Research* **21**, 557–567.

Haney, J. M., Nilvéus, R. E., McMillan, P. J. & Wikesjö, U. M. E. (1993) Periodontal repair in dogs: expanded polytetrafluoroethylene barrier membranes support wound stabilization and enhance bone regeneration. *Journal of Periodontology* **64**, 883–890.

Holmes, R. E. (1979) Bone regeneration within a coralline hydroxyapatite implant. *Plastic and Reconstructive Surgery* **63**, 626–633.

Koo, K. T., Polimeni, G., Albandar, J. M. & Wikesjö, U. M. E. (2004) Periodontal repair in dogs: examiner reproducibility in the supraalveolar periodontal defect model. *Journal of Clinical Periodontology* **31**, 439–442.

Kujala, S., Raatikainen, T., Ryhanen, J., Kaarela, O. & Jalovaara, P. (2002) Composite implant of native bovine bone morphogenetic protein (BMP) and biocoral in the treatment of scaphoid nonunions – a preliminary study. *Scandinavian Journal of Surgery* **91**, 186–190.

Mellonig, J. T. (1996) Bone allografts in periodontal therapy. *Clinical Orthopaedics and Related Research* **324**, 116–125.

Moon, I. S., Chai, J. K., Cho, K. S., Wikesjö, U. M. & Kim, C. K. (1996) Effects of polyglactin mesh combined with resorbable calcium carbonate or replamineform hydroxyapatite on periodontal repair in dogs. *Journal of Clinical Periodontology* **23**, 945–951.

Nasr, H. F., Aichelmann-Reidy, M. E. & Yukna, R. A. (1999) Bone and bone substitutes. *Periodontology 2000* **19**, 74–86.

Piattelli, A., Podda, G. & Scarano, A. (1997) Clinical and histological results in alveolar ridge enlargement using coralline calcium carbonate. *Biomaterials* **18**, 623–627.

Polimeni, G., Koo, K-T., Qahash, M., Xiropaidis, A. V., Albandar, J. M. & Wikesjö, U. M. E. (2004) Prognostic factors for alveolar regeneration: effect of a space-providing biomaterial on guided tissue regeneration. *Journal of Clinical Periodontology* **31**, 725–729.

Sigurdsson, T. J., Hardwick, R., Bogle, G. C. & Wikesjö, U. M. E. (1994) Periodontal repair in dogs: space provision by reinforced ePTFE membranes enhances bone and cementum regeneration in large supraalveolar defects. *Journal of Periodontology* **65**, 350–356.

Tatakis, D. N., Wikesjö, U. M. E., Razi, S. S., Sigurdsson, T. J., Lee, M. B., Nguyen, T., Ongpipattanakul, B. & Hardwick, R. (2000) Periodontal repair in dogs: effect of transforming growth factor-β1 on alveolar bone and cementum regeneration. *Journal of Clinical Periodontology* **27**, 698–704.

Tinti, C. & Vincenzi, G. P. (1994) expanded polytetrafluoroethylene titanium reinforced membranes for regeneration of mucogingival recession defects. A 12-case report. *Journal of Periodontology* **65**, 1088–1094.

Trombelli, L., Lee, M. B., Promsudthi, A., Guglielmoni, P. G. & Wikesjö, U. M. E. (1999) Periodontal repair in dogs: histologic observations of guided tissue regeneration with a prostaglandin E_1 analog/methacrylate composite. *Journal of Clinical Periodontology* **26**, 381–387.

Tuominen, T., Jamsa, T., Tuukkanen, J., Nieminen, P., Lindholm, T. C., Lindholm, T. S. & Jalovaara, P. (2000) Native bovine bone morphogenetic protein improves the potential of biocoral to heal segmental canine ulnar defects. *International Orthopaedics* **24**, 289–294.

Wikesjö, U. M. E., Kean, C. J. C. & Zimmerman, G. J. (1994) Periodontal repair in dogs: supraalveolar defect models for evaluation of safety and efficacy of periodontal reconstructive therapy. *Journal of Periodontology* **5**, 1151–1157.

Wikesjö, U. M. E., Lim, W. H., Razi, S. S., Sigurdsson, T. J., Lee, M. B., Tatakis, D. N. & Hardwick, W. R. (2003a) Periodontal repair in dogs: a bioresorbable calcium carbonate coral implant enhances space provision for alveolar bone regeneration in conjunction with guided tissue regeneration. *Journal of Periodontology* **74**, 955–962.

Wikesjö, U. M. E., Lim, W. H., Thomson, R. C., Cook, A. D., Wozney, J. M. & Hardwick, W. R. (2003b) Periodontal repair in dogs: evaluation of a bioresorbable space-providing macro-porous membrane with recombinant human bone morphogenetic protein-2. *Journal of Periodontology* **74**, 635–647.

Wikesjö, U. M. E., Lim, W. H., Thomson, R. C. & Hardwick, W. R. (2003c) Periodontal repair in dogs: gingival tissue occlusion, a critical requirement for guided tissue regeneration? *Journal of Clinical Periodontology* **30**, 655–664.

Wikesjö, U. M. E., Razi, S. S., Sigurdsson, T. J., Tatakis, D. N., Lee, M. B., Ongpipattanakul, B., Nguyen, T. & Hardwick, R. (1998) Periodontal repair in dogs: effect of recombinant human transforming growth factor $beta_1$ on guided tissue regeneration. *Journal of Clinical Periodontology* **25**, 475–481.

Wikesjö, U. M. E. & Nilvéus, R. (1991) Periodontal repair in dogs: healing patterns in large circumferential periodontal defects. *Journal of Clinical Periodontology* **18**, 49–59.

Wikesjö, U. M. E., Xiropaidis, A. V., Thomson, R. C., Cook, A. D., Selvig, K. A. & Hardwick, W. R. (2003d) Periodontal repair in dogs: rhBMP-2 significantly enhances bone formation under provisions for guided tissue regeneration. *Journal of Clinical Periodontology* **30**, 705–714.

Address:
Ki-Tae Koo
Laboratory for Applied Periodontal and Craniofacial Regeneration
Temple University School of Dentistry
Department of Periodontology
3223 North Broad Street
Philadelphia, PA 19140, USA
E-mail: wikesjo@comcast.net